Supporting Information

Measurement of Electric Fields Experienced by Urea Guest Molecules in the 18–Crown–6:Urea (1:5) Host–Guest Complex: An Experimental Reference Point for Electric-Field-Assisted Catalysis.

Ming W. Shi,[†] Sajesh P. Thomas,[†] Venkatesha R. Hathwar,[‡§] Alison J. Edwards,[¶] Ross O. Piltz,[¶] Dylan Jayatilaka,[†] George A. Koutsantonis,[†] Jacob Overgaard,[‡] Eiji Nishibori,[§] Bo B. Iversen,[‡] and Mark A. Spackman[†*]

[†] School of Molecular Sciences, University of Western Australia, 35 Stirling Highway, Crawley, WA 6009, Australia.

[‡] Center for Materials Crystallography and Department of Chemistry, Aarhus University, Langelandsgade 140, DK–8000 Aarhus C, Denmark.

[§] Division of Physics, Faculty of Pure and Applied Sciences, University of Tsukuba, 1–1–1 Tennodai, Tsukuba, Ibaraki 305–8571, Japan.

[¶] Australian Nuclear Science and Technology Organization, Australian Centre for Neutron Scattering, New Illawarra Road, Lucas Heights, New South Wales 2234, Australia.

Corresponding Author

*Mark Spackman (mark.spackman@uwa.edu.au)

Table of Contents

List of Tables

List of Figures

Relationship between 18C6:5U and urea inclusion compounds (UICs)

In **Figure S5** the projection of the folded urea layer in 18C6:5U is compared with projections of the hydrogen bonded urea networks in three UICs for which neutron diffraction structures were recently reported.[1] In the UIC with hexadecane (U:HEX, **Figure S5(b)**) the guest molecules are disordered and incommensurate with the urea host network, which is the hexagonal channel structure, often referred to as β-urea, common to UICs with an incommensurate guest structure. For the UICs with 1,6-dibromohexane (U:DBH) and 2,7-octanedione (U:OCT) in **Figure S5** the guests are ordered and commensurate with the urea network, which is slightly distorted from ideal hexagonal in U:DBH in order to accommodate the extended 1,6-dibromohexane molecule. Although the urea network in U:OCT has ideal hexagonal symmetry the tunnel walls are clearly distorted to a much greater extent (**Figure S5(d)**), with one of the four independent urea molecules forming a bridge between adjacent tunnels via N–H(syn)···O=C hydrogen bonds to two different guest molecules.

There is a simple relationship between the urea networks in 18C6:5U and U:HEX. Cleavage of that in U:HEX in the *ac* plane (i.e., perpendicular to **Figure S5(b)**), followed by appropriate translation in the *ab* plane results in a simpler version of the urea network found in 18C6:5U. **Figure S6** depicts the result of these operations with an overlay of the top and bottom halves of the network in U:HEX superimposed on the same projection of 18C6:5U in **Figure S5(a)**. The urea networks in the two structures are almost identical: the periodicity of the network in U:HEX along its a axis is 8.153 Å, while that for 18C6:5U along its b axis is 8.250 Å, and the angle between folds of ~125° in 18C6:5U is slightly greater than in U:HEX (exactly 120°). In support of this hypothetical process we note that the first report of the crystal structure of U:HEX[2] commented that "The crystals cleave quite readily along the *ac* plane but fracture if attempts are made to cleave them along the 001 plane or along other directions". The structure of this co-crystal between 18C6 and urea brings to mind the "Zebra Question":[3] Is it a structure formed by two 18C6:(urea)$_2$ trimers, stitched together with urea molecules, or a dislocated β-urea network alternating with 18C6 molecules, which form hydrogen bonds with urea molecules on both sides of the crown, acting as tethers holding the urea layers together?

Conformation of the crown ether molecules

The 'biangular' conformation of the crown ether molecules in 18C6:5U was identified in an early molecular mechanics study as one of the lowest energy conformations in the gas phase; other low-lying structures included the different C_i conformer found in the crystal of uncomplexed 18C6, and the highly symmetric D_{3d}.[4] More recent ab initio calculations[5] on gas phase structures did not locate the C_i conformer observed in 18C6:5U as a stable minimum, but indicated that the C_i conformer observed in the uncomplexed crystal lies ~8 kJ mol^{-1} above a still lower energy S_6 conformer, but ~25 kJ mol^{-1} below the D_{3d} conformer. This suggests that the present C_i conformer is not favorable in isolation, and adopted here because of the strong hydrogen bonds formed between urea *anti* H atoms and *adjacent* oxygen atoms of the crown (a 1,2 bridge). Our B3LYP-D3BJ/6-31+G(2df,p) calculations estimate the rearrangement energy between the D_{3d} and these observed C_i conformations to be ~36 kJ mol^{-1}, placing it well above the 47 unique lowest energy conformations described in reference [5].

Pyramidalization of urea nitrogens

In the gas phase urea is known to be "almost planar but … the amino groups are somewhat pyramidal".[6] Crystal structures derived from neutron diffraction data provide detailed information on hydrogen atom positions, which can be used to quantify the deviation of urea nitrogen atoms from the planar structure found in urea itself, where the molecule has ideal C_{2v} symmetry.[7] The present neutron structure of 18C6:5U, containing five urea molecules devoid of symmetry, reveals a wealth of information on the pyramidal nature of the amino nitrogen atoms. Here we use the angle between C–N–H$_{syn}$ and C–N–H$_{anti}$ planes as a measure of pyramidalization for each N atom. The values range from 2.5° to 17.9°, with a mean of 10.1° (**Table S5**). For the UIC neutron structures reported by Lee *at al.*[1] the average values are 4.6° (U:HEX, one unique N atom); 7.6° (U:OCT, range 0.7° to 12.5°, 7 unique N atoms); and 11.9° (U:DBH, range 2.1° to 23.8°, 6 unique N atoms). In all cases inspection of the structure reveals that the deviation of each H atom from the plane of the heavy atoms correlates with a close approach to an acceptor carbonyl oxygen atom. The uppermost values for 18C6:5U, U:OCT and U:DBH are all greater than found for urea amino nitrogens in other co-crystals for which neutron structures are available.[8]

Electron density topological parameters of the urea molecules

We focus initially on the mean values of ρ_{bcp} and $\nabla^2\rho_{bcp}$ for intramolecular bonds (**Table S3**), and their comparison with relevant literature results for urea in other crystal environments, namely urea itself,[9] and in its co-crystals with oxalic and L-malic acid.[10] Present values of ρ_{bcp} agree well – and within respective experimental errors – with those reported by Birkedal *et al.* for urea: 2.72(1) for C=O, 2.36(2) for C–N and 2.27(2) e Å^{-3} for N–H, but they are somewhat greater than the results obtained for urea in its co-crystals. Similar agreement with these previous studies is also observed for $\nabla^2\rho_{bcp}$, although more realistic esds of at least 2 e Å^{-5} need to be considered when comparing different experimental estimates of this quantity (see **Table S3** and discussion below).

From the plots in **Figure S9** and the higher R^2 values for C=O and C–N bonds it is clear that ρ_{bcp} is adequately described by a linear decrease with increasing bond length over this narrow range of bond distances. Although the scatter of the data is greater than the experimental esds for other bond types, **Table S3** also reveals that the esds from the inverse covariance matrix are sensible estimates of the reproducibility of ρ_{bcp} for N–H and C–H bonds, but underestimates for C–O and C–C. The situation for the Laplacian is completely different. The low values of R^2 for all bond types indicate there is no sensible relationship of these with bond length. Moreover, the experimental esds are at least an order of magnitude smaller than the standard deviation from the mean of the distribution for all bond types, indicating that the experimental esds systematically underestimate the true errors in that quantity.

The statistics in **Table S3** and the plots in **Figure S9** show that the experimental esds reported by the XD multipole modeling program are usually sensible estimates of the reproducibility of ρ_{bcp}, but an order of magnitude too small for $\nabla^2\rho_{bcp}$, a discrepancy that has also been noted recently by Krause et al.[11]

The search for intermolecular bcps yielded all N–H···O hydrogen bonds, as well as three C–H···π interactions and three H···H interactions (relevant geometric data and topological properties are listed in Table S4 in SI). Scatter diagrams of ρ_{bcp} and $\nabla^2\rho_{bcp}$ at N–H···O noncovalent bcps (**Figure S10**) show the expected correlation between intermolecular ρ_{bcp} and H···O distance in 18C6:5U, consistent with previous analyses.[12]

Table S1. Crystallographic details and refinement results for 18C6:5U.

Chemical formula	$(C_6H_{12}O_3)_2$: $(CH_4N_2O)_5$	
Crystal system, space group	Monoclinic, $P2_1/c$	
a, b, c (Å), β (°)	17.8250(3), 8.25020(10), 20.6233(4), 108.527(8)	
V (Å^3)	2875.68(6)	
Z	4	
Data collection	**Synchrotron**	**Neutron**
T (K)	30	30
Wavelength (Å)	0.24783	Laue
Crystal size	0.08 × 0.12 × 0.13 mm^3	0.6 × 0.6 × 1.6 mm^3
Completeness	99.9%	82.4%
N_{measured}, N_{unique}	163389, 47042	194702, 11494
R_{int} [a]	2.14 %	6.0 (4.5) %
$(\sin\theta/\lambda)_{\max}$ (Å^{-1})	1.25	0.83
Independent atom model refinement	**Synchrotron**	**Neutron**
Refinement on	F^2 (for $F > 4\sigma(F)$)	F (for $F > 3\sigma(F)$)
R, R_{all}, wR, S [b]	2.75, 3.52, 8.54, 1.029	4.99, 9.49, 3.71, 0.931
N, P	39591, 519	7840, 739
Deepest hole and highest peak in the difference Fourier map	–0.35, 0.66 e Å^{-3}	–1.95, 1.81 fm Å^{-3}
Multipole refinements	**MM–NEUTRON**	**MM–SHADE**
Refinement on	F^2	F^2
$R[F > 3\sigma(F)]$, wR, S	1.45, 3.6, 0.997	1.46, 1.77, 1.009
N, P	37623, 1350	37623, 1692
$\Delta\rho_{\min}$, $\Delta\rho_{\max}$ (e Å^{-3})	–0.11, 0.18	–0.11, 0.17

[a] $R_{\text{int}} = \sum_h \left| F^2_{h,\text{obs}} - \left\langle F^2_{h,\text{obs}} \right\rangle \right| / \sum_h F^2_{h,\text{obs}}$. For the neutron refinement R_{int} refers to the merge of normalized multiple wavelength data for 78247 reflections with $I > 4\sigma(I)$.

[b] $R(F) = 100 \cdot \sum_h \left\| F_{h,\text{obs}} \right| - \left| F_{h,\text{calc}} \right\| / \sum_h \left| F_{h,\text{obs}} \right|$, $wR(F) = 100 \cdot \left[\sum_h w_h \left(\left| F_{h,\text{obs}} \right| - \left| F_{h,\text{calc}} \right| \right)^2 / \sum_h w_h F^2_{h,\text{obs}} \right]^{1/2}$,

$S = \left[\sum_h \left(F^2_{h,\text{obs}} - F^2_{h,\text{calc}} \right)^2 / (N - P) \right]^{1/2}$ with $w_h = 1/\sigma^2_{h,\text{obs}}$, N the number of reflections and P the number of parameters.

Table S2. CE–B3LYP energy decomposition for unique nearest neighbor interactions in 18C6:5U and in the urea inclusion compound U:HEX. All energies are in kJ mol^{-1}. H_{anti} and H_{syn} denote H atoms on each urea molecule that are *anti* and *syn* to the C=O moiety, respectively. Separate energy terms are unscaled, and $E_{tot} = 1.057E_{ele} + 0.740E_{pol} + 0.871E_{dis} + 0.618E_{rep}$.[13]

	interaction	E_{ele}	E_{pol}	E_{dis}	E_{rep}	E_{tot}
urea 1	O+H_{syn}···urea2	–70.9	–17.5	–11.1	58.0	–61.7
	O+H_{syn} ···urea3	–81.2	–20.9	–13.7	73.3	–68.0
	O···urea3	–40.6	–10.8	–9.2	43.7	–32.0
	H_{anti}+H_{anti}···crown1	–67.0	–18.6	–38.2	63.0	–78.9
urea 2	O···urea3	–32.6	–9.4	–7.8	33.4	–27.5
	O+H_{syn}···urea4	–72.1	–17.5	–12.4	61.7	–61.8
	H_{anti}···urea3	–40.5	–10.3	–6.9	38.3	–32.8
	H_{anti}···urea5	–23.5	–7.6	–7.9	20.0	–24.9
urea 3	O+H_{syn}···urea5	–70.6	–17.9	–12.9	60.7	–61.6
urea 4	O+H_{syn}···urea5	–65.0	–15.7	–12.6	54.8	–57.5
	O···urea4 = H_{anti}···urea4	–32.7	–9.3	–7.1	31.1	–28.4
	H_{anti}···urea5	–32.6	–8.8	–6.4	25.8	–30.7
urea 5	H_{anti}+H_{anti}···crown2	–69.5	–19.6	–38.1	68.6	–78.8
U:HEX	O+Hsyn···urea_a	–63.7	–15.7	–12.4	48.0	–60.2
	O···urea_b	–32.2	–9.1	–7.2	28.3	–29.6

Table S3. Linear regression analysis of topological properties of the experimental electron density at covalent and N–H···O noncovalent bcps.

ρ_{bcp}, e Å^{-3}	R^2	mean	experimental mean esd[a]	esd in model[b]
C=O	0.92	2.776	0.013	0.011
C–N	0.78	2.444	0.011	0.016
N–H	0.45	2.291	0.028	0.024
C–O	0.16	1.873	0.011	0.029
C–C	0.54	1.896	0.010	0.016
C–H	0.08	1.863	0.028	0.033
N–H···O	0.91	0.155	0.013	0.018

$\nabla^2\rho_{bcp}$, e Å^{-5}	R^2	mean	experimental mean esd[a]	esd in model[b]
C=O	0.18	–35.00	0.08	1.38
C–N	0.01	–26.88	0.05	1.59
N–H	0.03	–34.62	0.18	2.02
C–O	0.07	–15.32	0.04	1.43
C–C	0.46	-17.59	0.03	0.78
C–H	0.01	–20.62	0.12	1.26
N–H···O	0.93	1.72	0.02	0.16

[a] mean of experimental esds from inverse of the variance-covariance matrix

[b] estimated standard deviation of error in the model from linear regression analysis

Table S4. Topological properties at bond critical points for the covalent bonds in 18C6:5U **(**MM–NEUTRON model**).**

bond	bond distance /Å	ρ_{bcp}/e Å^{-3}	$\nabla^2\rho_{\mathrm{bcp}}$/e Å^{-5}	ϵ
		Urea		
C1–O1	1.2649 (2)	2.74 (1)	–33.60 (8)	0.14
C2–O2	1.2597 (1)	2.80 (1)	–36.27 (8)	0.09
C3–O3	1.2615 (1)	2.78 (1)	–33.59 (7)	0.10
C4–O4	1.2579 (1)	2.82 (1)	–36.10 (8)	0.11
C5–O5	1.2684 (2)	2.74 (1)	–35.39 (7)	0.12
C1–N1	1.3391 (1)	2.48 (1)	–25.47 (5)	0.19
C1–N2	1.3466 (1)	2.44 (1)	–28.98 (5)	0.19
C2–N3	1.3439 (1)	2.49 (1)	–28.30 (5)	0.18
C2–N4	1.3528 (1)	2.41 (1)	–24.94 (5)	0.18
C3–N5	1.3415 (1)	2.48 (1)	–25.40 (5)	0.18
C3–N6	1.3503 (1)	2.42 (1)	–26.61 (5)	0.20
C4–N7	1.3495 (1)	2.40 (1)	–26.23 (5)	0.23
C4–N8	1.3481 (1)	2.44 (1)	–28.48 (5)	0.18
C5–N9	1.3415 (1)	2.47 (1)	–28.35 (5)	0.24
C5–N10	1.3456 (1)	2.44 (1)	–25.99 (5)	0.20
N1–H1s	1.0150 (1)	2.26 (3)	–33.6 (2)	0.08
N1–H1a	1.0116 (1)	2.32 (3)	–37.1 (2)	0.08
N2–H2s	1.0149 (1)	2.26 (3)	–31.0 (2)	0.05
N2–H2a	1.0075 (1)	2.34 (3)	–35.6 (2)	0.05
N3–H3s	1.0188 (1)	2.22 (3)	–33.7 (2)	0.04
N3–H3a	1.0138 (1)	2.28 (3)	–34.4 (2)	0.04
N4–H4s	1.0142 (1)	2.31 (3)	–38.1 (2)	0.04
N4–H4a	1.0125 (1)	2.31 (3)	–30.5 (2)	0.05
N5–H5s	1.0189 (1)	2.25 (3)	–36.2 (2)	0.04
N5–H5a	1.0162 (1)	2.30 (3)	–35.9 (2)	0.04
N6–H6s	1.0084 (1)	2.28 (3)	–36.6 (2)	0.03
N6–H6a	1.0129 (1)	2.32 (3)	–36.2 (2)	0.03
N7–H7s	1.0208 (1)	2.27 (3)	–33.6 (2)	0.05
N7–H7a	1.0097 (1)	2.29 (3)	–32.9 (2)	0.07
N8–H8s	1.0209 (1)	2.27 (3)	–33.5 (2)	0.07
N8–H8a	1.0107 (1)	2.34 (3)	–34.2 (2)	0.04
N9–H9s	1.0162 (1)	2.27 (3)	–32.6 (2)	0.03
N9–H9a	1.0176 (1)	2.29 (3)	–36.5 (2)	0.06
N10–H10s	1.0080 (1)	2.32 (3)	–34.9 (2)	0.08
N10–H10a	1.0114 (1)	2.33 (3)	–35.3 (2)	0.05
		18–crown–6		
C6–O6	1.4203 (2)	1.88 (1)	–14.50 (4)	0.05
C7–O6	1.4203 (2)	1.86 (1)	–15.61 (4)	0.09
C9–O7	1.4201 (2)	1.83 (1)	–15.59 (4)	0.04
C10–O8	1.4198 (2)	1.86 (1)	–15.31 (4)	0.13
C11–O8	1.4251 (2)	1.88 (1)	–17.81 (4)	0.09

C12–O9	1.4121 (2)	1.93 (1)	–15.59 (4)	0.02
C13–O9	1.4175 (2)	1.83 (1)	–14.64 (4)	0.05
C14–O10	1.4180 (2)	1.91 (1)	–16.68 (4)	0.05
C15–O10	1.4245 (2)	1.86 (1)	–14.83 (4)	0.06
C16–O11	1.4190 (2)	1.86 (1)	–12.89 (4)	0.06
C6–C11	1.5140 (2)	1.87 (1)	–16.40 (3)	0.02
C7–C8	1.5060 (2)	1.90 (1)	–17.70 (3)	0.06
C9–C10	1.5071 (2)	1.91 (1)	–18.77 (3)	0.05
C12–C17	1.5063 (2)	1.90 (1)	–17.25 (3)	0.04
C13–C14	1.5088 (2)	1.93 (1)	–18.57 (3)	0.04
C15–C16	1.5143 (2)	1.87 (1)	–16.83 (3)	0.10
C6–H61	1.1037 (1)	1.92 (3)	–20.0 (1)	0.06
C6–H62	1.1042 (1)	1.92 (3)	–21.8 (1)	0.02
C7–H71	1.1069 (1)	1.86 (3)	–21.8 (1)	0.08
C7–H72	1.1016 (1)	1.88 (3)	–20.4 (1)	0.06
C8–H81	1.1036 (1)	1.89 (3)	–21.4 (1)	0.05
C8–H82	1.1064 (1)	1.88 (3)	–22.7 (1)	0.06
C9–H91	1.1007 (1)	1.86 (3)	–21.3 (1)	0.05
C9–H92	1.1023 (1)	1.85 (3)	–20.8 (1)	0.06
C10–H101	1.0957 (1)	1.88 (3)	–19.6 (1)	0.04
C10–H102	1.1036 (1)	1.84 (3)	–20.3 (1)	0.06
C11–H111	1.0981 (1)	1.86 (3)	–21.6 (1)	0.03
C11–H112	1.0964 (1)	1.90 (3)	–22.8 (1)	0.06
C12–H121	1.1033 (1)	1.85 (3)	–20.8 (1)	0.04
C12–H122	1.1075 (1)	1.86 (3)	–20.1 (1)	0.05
C13–H131	1.1051 (1)	1.82 (3)	–19.0 (1)	0.09
C13–H132	1.1027 (1)	1.83 (3)	–20.3 (1)	0.07
C14–H141	1.1032 (1)	1.81 (3)	–20.0 (1)	0.1
C14–H142	1.0958 (1)	1.91 (3)	–21.2 (1)	0.05
C15–H151	1.0957 (2)	1.88 (3)	–21.9 (1)	0.11
C15–H152	1.1054 (1)	1.82 (3)	–19.9 (1)	0.04
C16–H161	1.1000 (1)	1.85 (3)	–18.3 (1)	0.04
C16–H162	1.1076 (1)	1.88 (3)	–21.3 (1)	0.05
C17–H171	1.1027 (1)	1.79 (3)	–18.0 (1)	0.05
C17–H172	1.1007 (1)	1.87 (3)	–19.7 (1)	0.07

Table S5. Topological properties at bond critical points for the noncovalent interactions in 18C6:5U (MM–NEUTRON model)

hydrogen bond	d(D–H) Å	d(H···A) Å	d(D–A) Å	Angle °	ρ_{bcp} e Å^{-3}	$\nabla^2\rho_{\mathrm{bcp}}$ e Å^{-5}	C–N–H angle[#] °
N1–H1s···O3’	1.015(3)	1.907	2.921(1)	176.3(2)	0.19 (1)	1.9 (2)	5.7
N1–H1a···O10	1.012(2)	1.922	2.884(1)	157.7(3)	0.18 (1)	1.9 (3)	
N2–H2s···O2	1.007(2)	2.291	3.199(1)	149.3(3)	0.12 (1)	1.8 (2)	6.4
N2–H2a···O11	1.015(2)	1.998	3.001(1)	169.3(2)	0.07 (1)	0.8 (1)	
N3–H3s···O1	1.018(2)	1.897	2.908(1)	171.5(2)	0.19 (1)	1.9 (2)	18.5
N3–H3a···O3’	1.013(3)	1.865	2.875(1)	173.7(2)	0.19 (1)	2.0 (3)	
N4–H4s···O4	1.016(3)	1.998	3.004(1)	170.2(2)	0.14 (1)	1.3 (2)	10.6
N4–H4a···O5	1.011(3)	2.084	3.033(1)	155.7(2)	0.09 (1)	1.7 (2)	
N5–H5s···O1	1.020(3)	1.893	2.911(1)	176.0(2)	0.17 (1)	1.9 (3)	2.5
N5–H5a···O1’	1.017(3)	1.860	2.870(1)	171.7(2)	0.20 (1)	2.0 (3)	
N6–H6s···O5	1.009(2)	2.011	3.016(1)	174.3(2)	0.14 (1)	1.4 (2)	13.1
N6–H6a···O2’	1.013(3)	1.937	2.900(1)	157.7(2)	0.14 (1)	1.9 (2)	
N7–H7s···O2	1.020(2)	1.888	2.903(1)	172.6(2)	0.16 (1)	2.3 (3)	15.2
N7–H7a···O5’	1.011(3)	1.980	2.968(1)	164.9(2)	0.15 (1)	1.7 (2)	
N8–H8s···O5	1.021(3)	1.905	2.915(1)	169.5(2)	0.17 (1)	1.9 (3)	8.9
N8–H8a···O4”	1.012(3)	1.938	2.914(1)	161.1(2)	0.17 (1)	1.9 (2)	
N9–H9s···O3	1.017(2)	1.892	2.906(1)	173.9(2)	0.21 (1)	1.8 (2)	17.9
N9–H9a···O8	1.017(3)	1.825	2.839(1)	174.0(2)	0.22 (2)	2.0 (3)	
N10–H10s···O4	1.009(3)	2.061	3.042(1)	163.3(2)	0.13 (1)	1.5 (2)	2.5
N10–H10a···O6	1.011(2)	2.324	3.263(1)	154.1(2)	0.08 (1)	0.7 (1)	
C16–H161···π(C1=O1)	1.102	2.589	3.624(1)	156.2(2)	0.05 (1)	0.6 (0)	–
C15–H152···π(C2=O2)	1.105	2.556	3.573(1)	152.5(2)	0.06 (0)	0.5 (0)	–
C6–H61··· π(C5=O5)					0.04 (1)	0.5 (0)	–
H161···H3s					0.02 (0)	0.4 (0)	–
H141···H4a					0.01 (0)	0.2 (0)	–
H101···H62					0.07 (1)	1.2 (0)	–

The angle between C–N–H_{syn} and C–N–H_{anti} planes is a measure of pyramidalization for each N atom (see text).

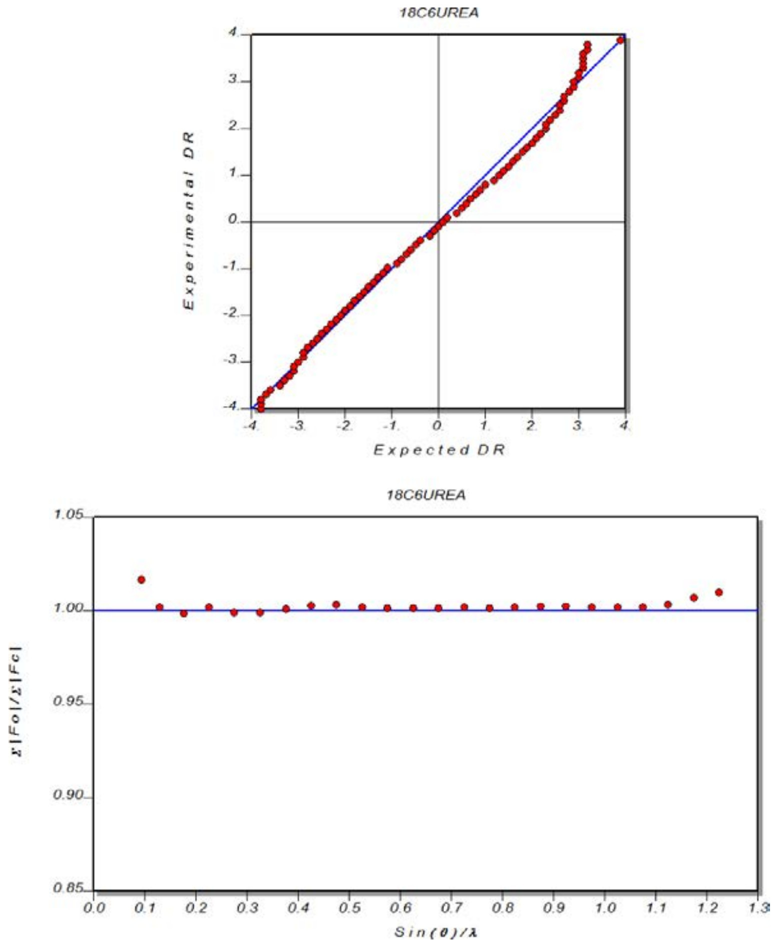

Figure S1. Normal probability plot (top) and distribution of average scale factors as a function of sinθ/λ (bottom) for the MM–NEUTRON model.

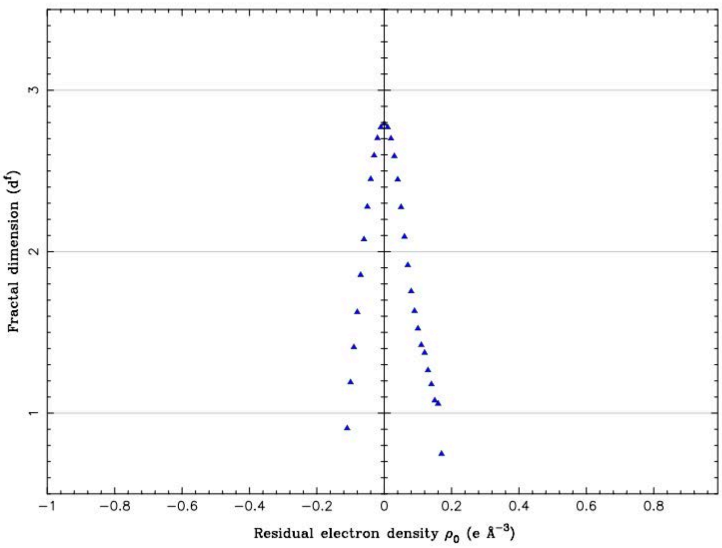

Figure S2. Fractal dimension plot for the MM–NEUTRON model.

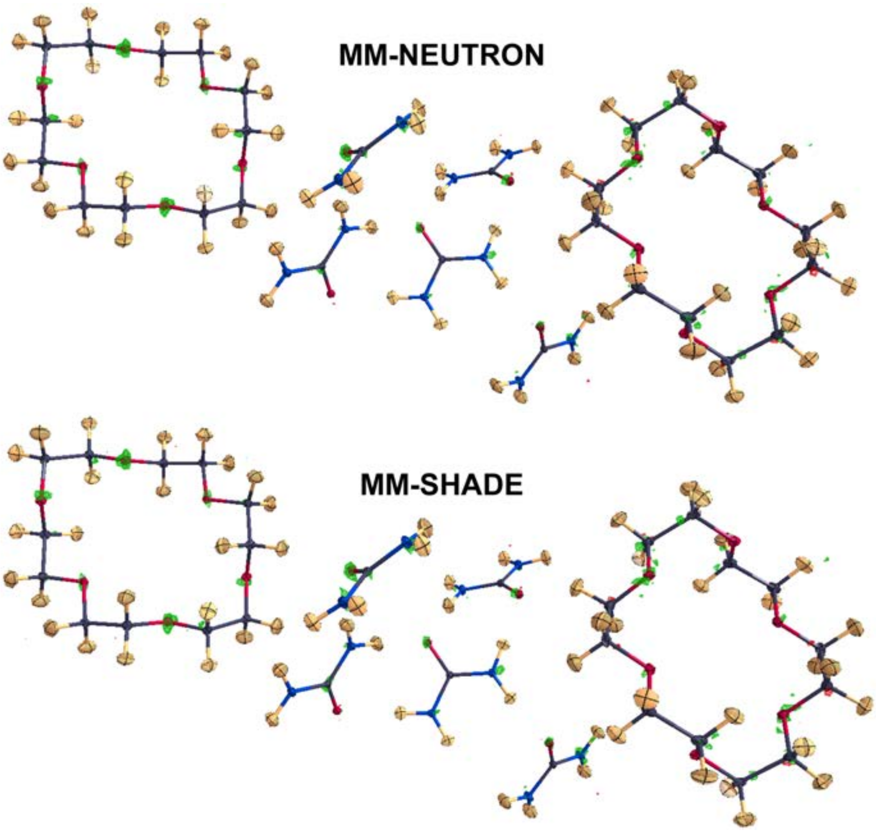

Figure S3. Residual electron density isosurface maps, $\Delta\rho_{residual}$, for MM–NEUTRON and MM–SHADE models. Isovalues are ±0.1 e Å^{-3} and positive/negative residual density surfaces are red/green.

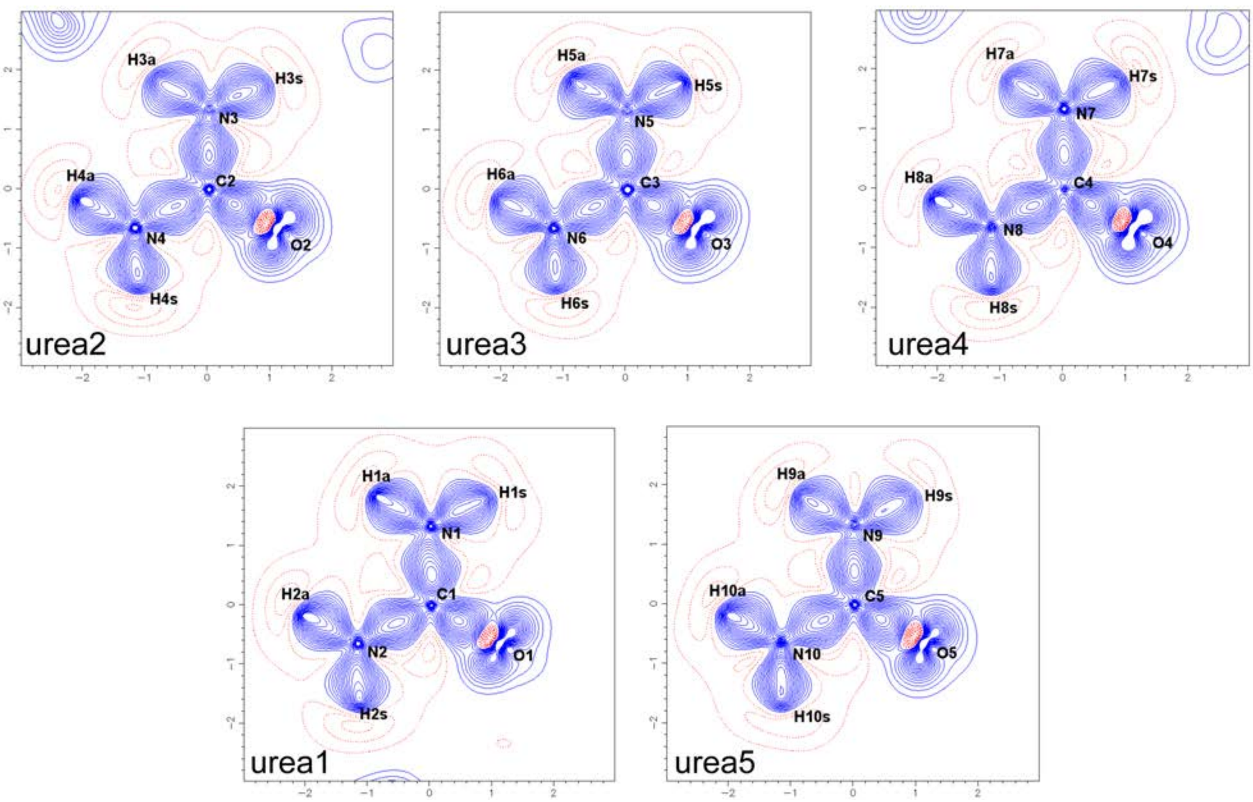

Figure S4. Static deformation electron density maps for urea molecules from the MM–NEUTRON model. Contour intervals are 0.05 e Å^{-3}. Blue solid lines are positive; red dotted lines are negative.

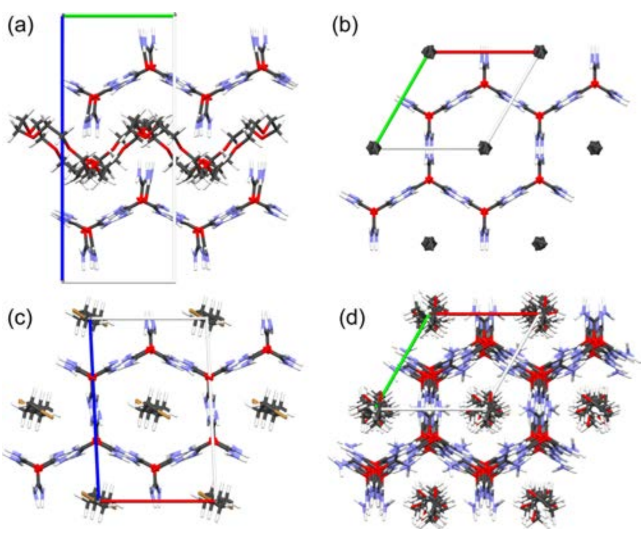

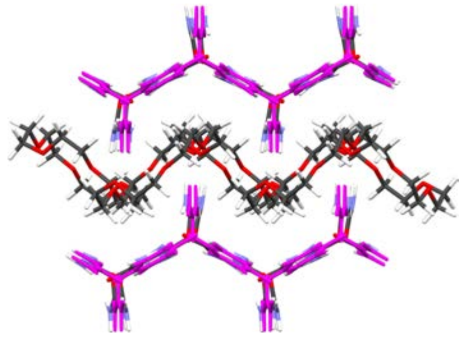

Figure S5. (a) Projection of the urea hydrogen bonding network in 18C6:5U, compared with those in urea inclusion compounds with: (b) hexadecane, U:HEX; (c) 1,6-dibromohexane, U:DBH; and (d) 2,7-octanedione, U:OCT. All structures are based on neutron diffraction data; guest molecules are disordered and incommensurate with the host network for (b), but ordered and commensurate in (c) and (d).[1]

Figure S6. Overlay of the upper and lower halves of the urea network in U:HEX (magenta) superimposed on the urea hydrogen bonding network in 18C6:5U.

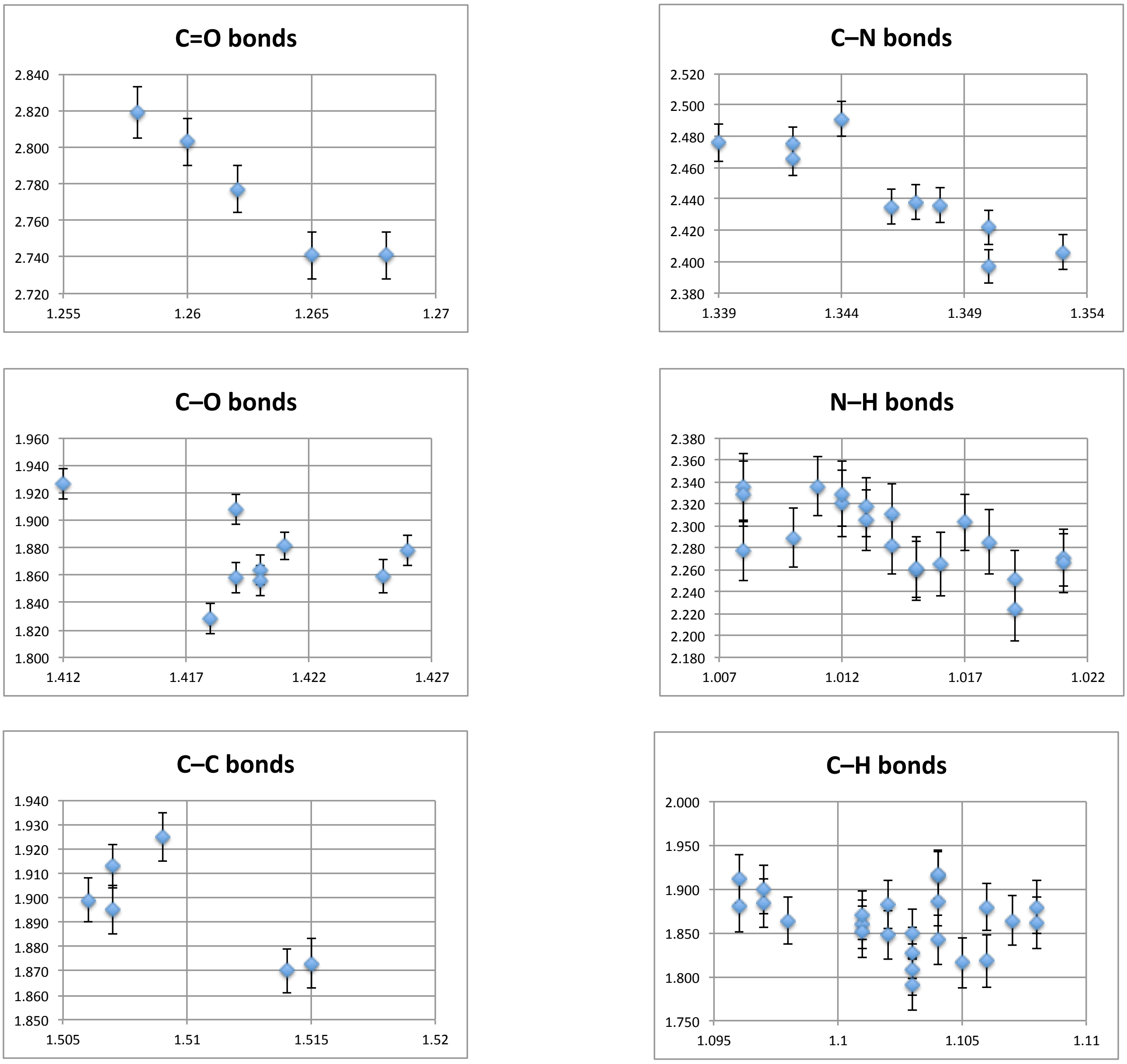

Figure S7. Scatter plots of electron density at bcps for covalent bonds in 18C6:5U. Error bar estimates from XD are ~0.01 e Å^{-3} for bonds between heavy atoms and ~0.03 e Å^{-3} for bonds to H atoms. Interatomic distances are in Å (horizontal axis) and all plots span the same range of 0.015 Å; electron density (vertical axis) in e Å^{-3}.

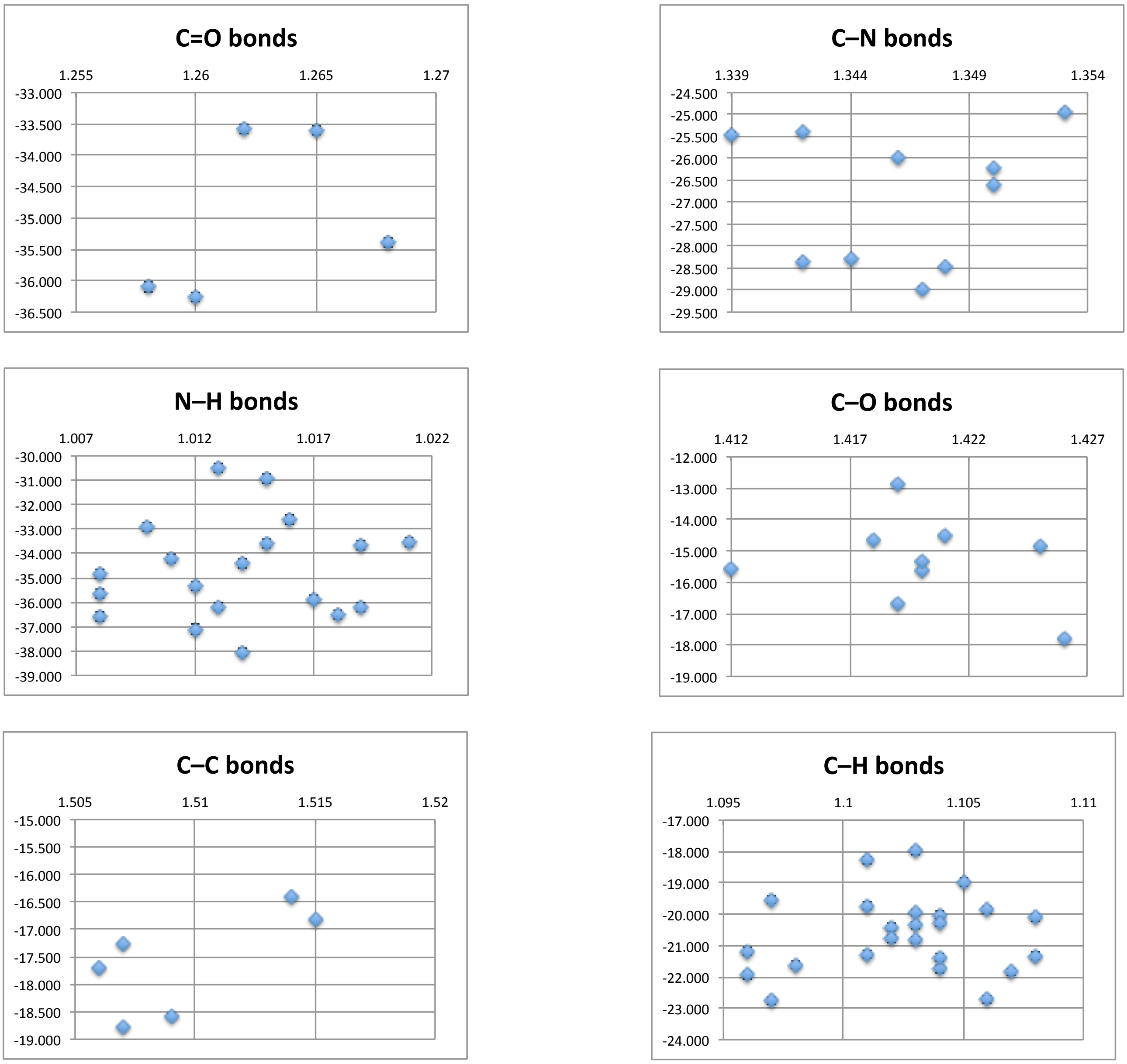

Figure S8. Scatter plots of Laplacian of the electron density at bcps for covalent bonds in 18C6:5U. Error bar estimates from XD are smaller than the size of the symbols in all cases. Interatomic distances are in Å (horizontal axis) and all plots span the same range of 0.015 Å; Laplacian of the electron density (vertical axis) in e Å^{-5}.

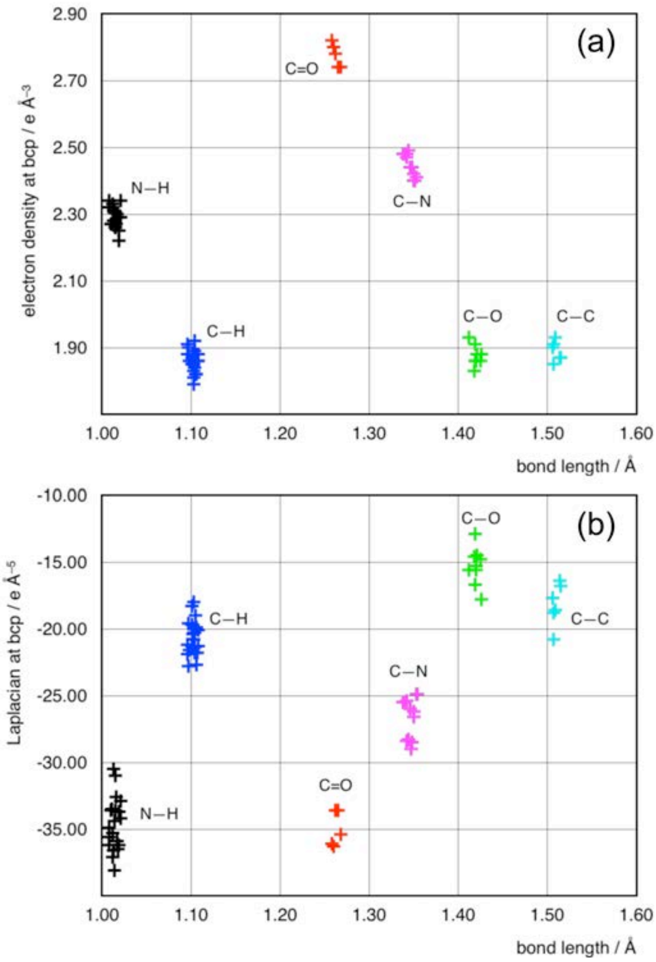

Figure S9. Scatter diagrams of (a) ρ_{bcp} and (b) $\nabla^2\rho_{bcp}$ at covalent bcps in 18C6:5U from the experimental electron density.

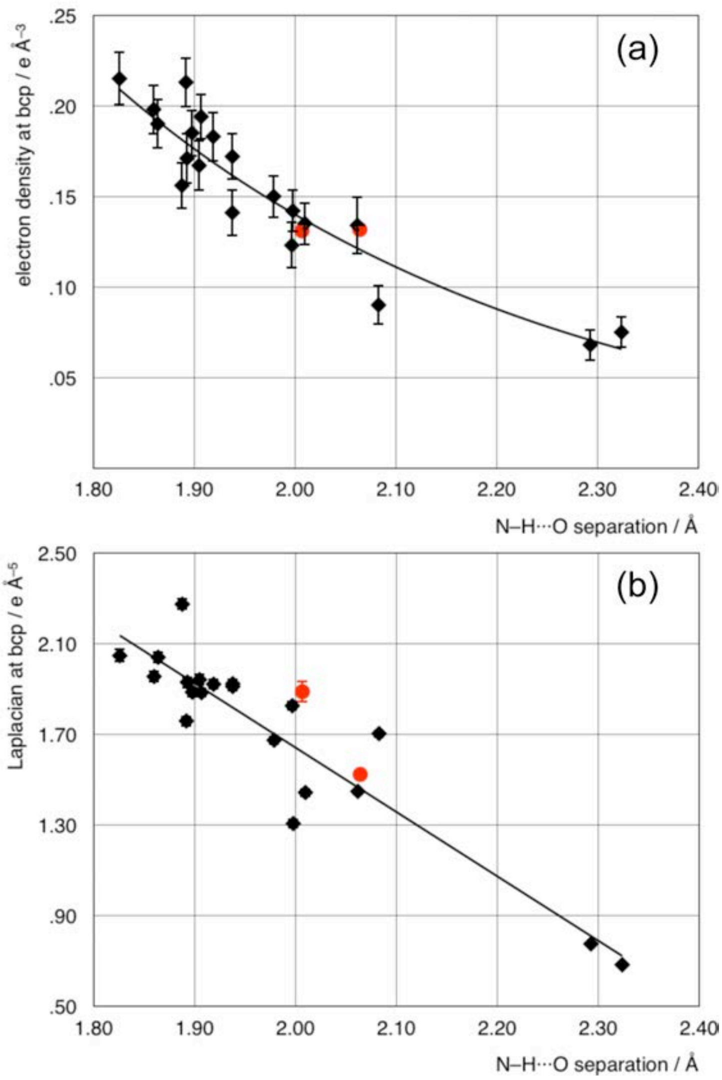

Figure S10. Scatter diagrams of (a) ρ_{bcp} and (b) $\nabla^2\rho_{bcp}$ at N–H···O noncovalent bcps (black diamonds) from the MM-NEUTRON electron density. Error bars are from the least squares multipole refinement, and in (b) they are smaller than the symbols. This shows the expected correlation between intermolecular ρ_{bcp} and H···O distance in 18C6:5U, consistent with previous analyses.[14] The exponential fit derived in that work (also based on neutron geometries), $\rho_{bcp}(R) = 8(4)\exp[-2.1(3)R]$, agrees very well with the present result [$\rho_{bcp}(R) = 14.6\exp(-2.33R)$]. Results for the two hydrogen bonds in crystalline urea[9] (filled red circles) were omitted from trendlines. The figure also shows that ρ_{bcp} and $\nabla^2\rho_{bcp}$ from the experimental charge density analysis of urea[9] are in excellent agreement with the present results.

References

(1) Lee, R.; Mason, S. A.; Mossou, E.; Lamming, G.; Probert, M. R.; Steed, J. W., Neutron Diffraction Studies on Guest-Induced Distortions in Urea Inclusion Compounds, *Cryst. Growth Des.* **2016**, *16*, 7175-7185.

(2) Smith, A. E., The crystal structure of the urea-hydrocarbon complexes, *Acta Crystallogr.* **1952**, *5*, 224-235.

(3) Silverstein, S. *A Light in the Attic*; Harper & Row: New York, 1981.

(4) Uiterwijk, J.; Harkema, S.; Feil, D., A molecular mechanics study of 18-crown-6 and its complexes with neutral organic-molecules, *J. Chem. Soc., Perkin Trans. 2* **1987**, 721-731.

(5) Al-Jallal, N. A.; Al-Kahani, A. A.; El-Azhary, A. A., Conformational Study of the Structure of Free 18-Crown-6, *J. Phys.*

Chem. A **2005**, *109*, 3694-3703.
(6) Godfrey, P. D.; Brown, R. D.; Hunter, A. N., The shape of urea, *J. Mol. Struct.* **1997**, *413-414*, 405-414.
(7) Swaminathan, S.; Craven, B. M.; McMullan, R. K., The Crystal Structure and Molecular Thermal Motion of Urea at 12, 60 and 123 K from Neutron Diffraction, *Acta Crystallogr., Sect. B: Struct. Sci.* **1984**, *40*, 300-306.
(8) Co-crystals with fumaric acid (TIPWIY02), hydrogen peroxide (UREXPO11), oxalic acid (1:1 UROXAM01); and 2:1 UROXAL01) and succinic acid (VEJXAJ02). The range of values is 2.4° to 10.8° with a mean of 5.9°.
(9) Birkedal, H.; Madsen, D.; Mathiesen, R. H.; Knudsen, K.; Weber, H. P.; Pattison, P.; Schwarzenbach, D., The charge density of urea from synchrotron diffraction data, *Acta Crystallogr., Sect. A: Found. Crystallogr.* **2004**, *60*, 371-381.
(10) Krawczuk, A.; Gryl, M.; Pitak, M. B.; Stadnicka, K., Electron Density Distribution of Urea in Co-crystals with Rigid and Flexible Dicarboxylic Acids, *Cryst. Growth Des.* **2015**, *15*, 5578-5592.
(11) Krause, L.; Niepötter, B.; Schürmann, C. J.; Stalke, D.; Herbst-Irmer, R., Validation of experimental charge-density refinement strategies: when do we overfit?, *IUCrJ* **2017**, *4*, 420-430.
(12) Espinosa, E.; Souhassou, M.; Lachekar, H.; Lecomte, C., Topological analysis of the electron density in hydrogen bonds, *Acta Crystallogr., Sect. B: Struct. Sci.* **1999**, *55*, 563-572.
(13) Mackenzie, C. F.; Spackman, P. R.; Jayatilaka, D.; Spackman, M. A., CrystalExplorer model energies and energy frameworks: Extension to metal coordination compounds, organic salts, solvates and open shell systems, *IUCrJ* **2017**, *4*, 575-587.
(14) Espinosa, E.; Souhassou, M.; Lachekar, H.; Lecomte, C., Topological analysis of the electron density in hydrogen bonds, *Acta Crystallogr. B* **1999**, *55*, 563-572.